Successful Applications of Computer Aided Drug Discovery: Moving Drugs from Concept to the Clinic

Tanaji T. Talele*[1], Santosh A. Khedkar[2] and Alan C. Rigby[2]

[1]*Department of Pharmaceutical Sciences, College of Pharmacy and Allied Health Professions, St. John's University, Jamaica, NY 11439,* [2]*Laboratory for Target Validation and Drug Discovery, Center for Vascular Biology Research, Division of Molecular and Vascular Medicine, Department of Medicine, Beth Israel Deaconess Medical Center, Harvard Medical School, Boston, MA 02215*

Abstract: Drug discovery and development is an interdisciplinary, expensive and time-consuming process. Scientific advancements during the past two decades have changed the way pharmaceutical research generate novel bioactive molecules. Advances in computational techniques and in parallel hardware support have enabled *in silico* methods, and in particular structure-based drug design method, to speed up new target selection through the identification of hits to the optimization of lead compounds in the drug discovery process. This review is focused on the clinical status of experimental drugs that were discovered and/or optimized using computer-aided drug design. We have provided a historical account detailing the development of 12 small molecules (Captopril, Dorzolamide, Saquinavir, Zanamivir, Oseltamivir, Aliskiren, Boceprevir, Nolatrexed, TMI-005, LY-517717, Rupintrivir and NVP-AUY922) that are in clinical trial or have become approved for therapeutic use.

Keywords: Molecular modeling, Structure-activity relationship, X-ray crystallography, Clinical trials, Success stories.

INTRODUCTION

Exponential explosion of structural information is the result of numerous structural genomic initiatives that have leveraged methodological advancements in high throughput X-ray crystallographic and/or NMR spectroscopy approaches that have been partnered with novel molecular biology cloning techniques. The rational design of novel drug-like candidates using structure-based drug design is a viable alternative to phenotypic high throughput screens (HTS) provided the structure of the therapeutic target protein has been determined by X-ray crystallography, NMR spectroscopy or generated using homology modeling techniques that are reliant upon the structural details of a family member. In structure-based drug design, structural data of the target receptor, preferably in complex with a ligand, is requisite in the discovery process. These structural data provide important structure-activity relationship (SAR) details of the therapeutic target of interest in a ligand-bound conformation. However, structural details gleaned from the structure of the target in the presence of several unique ligands provide important insight into the geometric fit of these compounds into the binding site and details including a low-energy conformation, ideal molecular electrostatic potentials, the presence of charged and/or neutral hydrogen bonds between functional groups, and hydrophobic interactions between lipophilic surfaces. While hydrophobic interactions increase receptor-ligand binding affinities, the contribution of hydrogen bonds to the overall binding free energy is dependent on a balance between desolvation energies of this interaction and the energy imparted on the system by newly formed hydrogen bonds.

*Address correspondence to this author at the Department of Pharmaceutical Sciences, College of Pharmacy and Allied Health Professions, St. John's University, Jamaica, NY 11439; E-mail: talelet@stjohns.edu

Subtle functional group alterations within the drug-like ligand can have complex structure-function consequences. Using sophisticated molecular modeling software, the ligand can be modified *in silico* to achieve a "better", theoretical fit between defined binding sites and complementary molecular volumes. In these studies the bound ligand is removed from the binding site of the receptor and new molecular structures are computationally docked into the binding site. Evidence of the successes of structure-based design efforts to drug development is reflected in the large number of new drug entities that are currently in clinical evaluation. The central assumption of structure-based drug design is that this is an iterative process, which involves multiple cycles of design and optimization with a singular goal of identifying a modulator (inhibitor, activator, agonist or antagonist) of the target enzyme or receptor. Ideally this drug-like compound would have demonstrable activity in the nanomolar concentration range, possess good selectivity, high binding affinity, significant ligand efficiency as well as acceptable pharmacokinetic properties. A typical *in silico* drug design cycle consists of docking, scoring and ranking initial hits on the basis of their steric and electrostatic interactions with the target site, which is commonly referred to as virtual screening (Fig. **1**). One alternate approach employs a ligand-based pharmacophore strategy that is often partnered with structure-based docking that uses a more stringent scoring matrix to enhance the enrichment of initial hits and identify the best compounds for biochemical evaluation, which are the 1st generation hits. In the second phase, the molecular interactions between the target and biologically validated hits/leads (per industry metrics of KD, IC_{50} or K_i) often identify ligand-based sites for optimizing these metrics for a unique molecular chemotype. In many situations, 2D similarity searches of databases are performed using chemotype information from the first generation hits. This approach

1568-0266/10 $55.00+.00

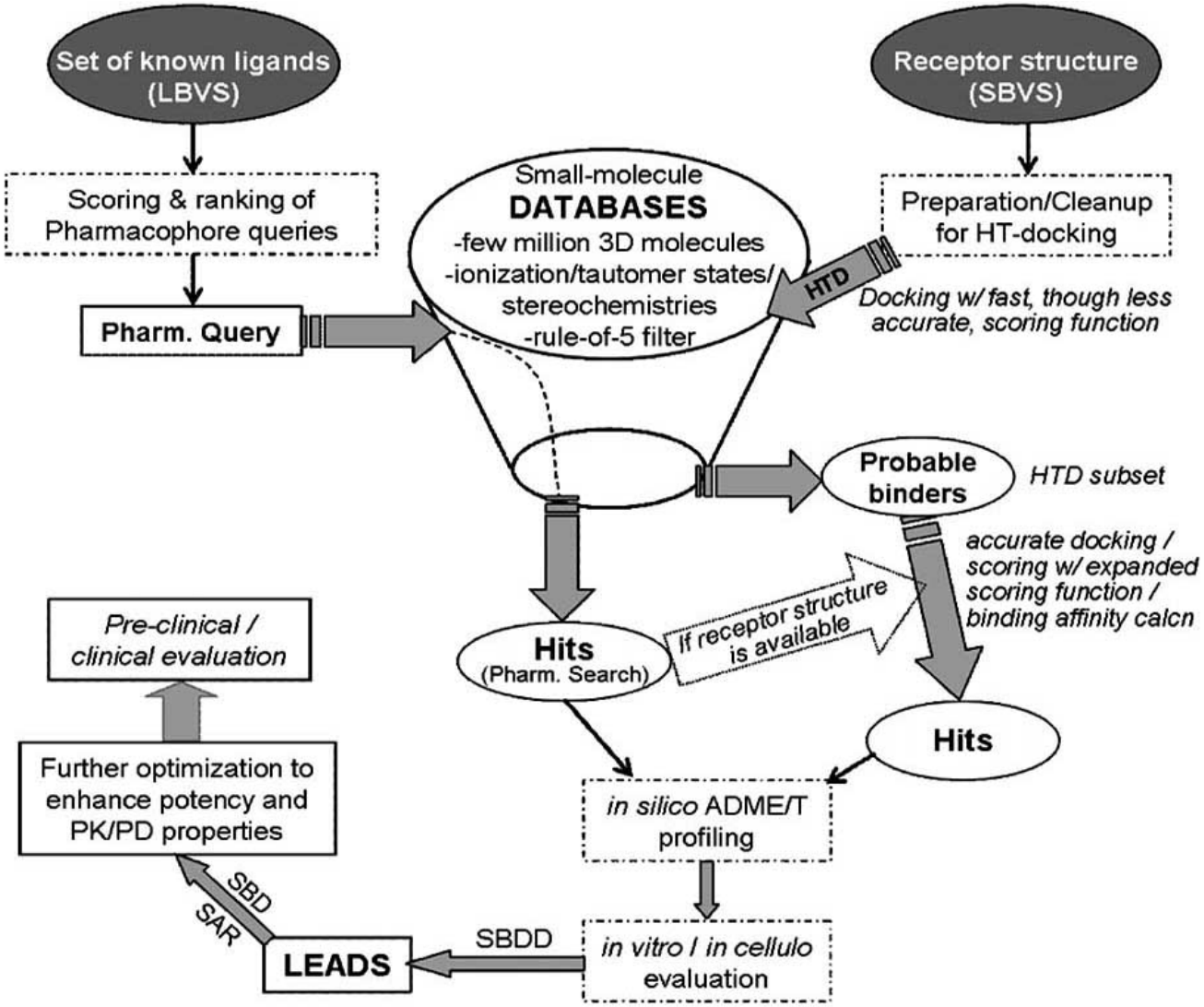

Fig. (1). Flow chart of a typical virtual screening and lead optimization program. Depending on the information available at the start of a discovery project, one may rely on knowledge of known ligands (LBVS) and/or on the structure of the target receptor (SBVS). The pharmacophore searches are relatively faster than high-throughput docking, and, combining results of both approaches is documented to yield better enrichment of actives. A relevant treatment of ligands in the databases such as stereochemistries and possible ionization and tautomer state at relevant pH conditions may help minimize the false negative rate (*i.e.*, missing of active molecule from the hit list). ADME/T evaluation of a small subset of hits before biological evaluation (*in vitro* or *in cellulo*) may help reduce late stage failures of hits or leads. Thorough structure-activity relationship (SAR) around the active hits may find a lead compound(s) which may be subjected to pre-clinical and clinical evaluations, including PK/PD optimization.

often identifies commercially available modifications of these lead compounds (limited SAR data), which are thoroughly evaluated computationally prior to being ordered and evaluated in a biological assay. Subsequent iterations of this process may necessitate the chemical synthesis of other commercially unavailable and/or novel modifications around the lead chemotype. Ultimately a lead optimized compound that is active *in vitro* and *in cellulo* is co-crystallized in the presence of the target to provide additional SAR information and permit structure-guided pharmacokinetic and pharmaco-dynamic optimization with the goal of reducing toxicity while improving potency. While this remains a highly iterative process, in silico structure-guided identification, design and optimization cycles significantly decrease the length of time needed to identify/develop optimized lead compounds that merit clinical evaluation.

The purpose of this review is to provide the reader with a historical overview on how coupling computational (structure- and/or ligand-based) design with a rational decision process has led to the discovery of small molecule therapeutic agents with activity directed against target proteins critical in the presentation of numerous disease conditions and/or have supported their clinical evaluation with several approved by the Food and Drug Administration (FDA). Given that it is a daunting task to provide all of the details articulating the role played by computational techniques in the evolution of each of these candidates to the clinic, we have guided the reader to the original references

for additional information. Given the theme of this special issue, we have limited the scope of this review to highlight the role computational techniques have played in these successes. Throughout the remainder of this special issue several other thought leaders within their respective field of computational discovery discuss recent advances in their respective field and how these advances have been successfully applied in recent drug design projects. Understanding the complexity and collaborative spirit needed to be successful in drug discovery, the authors of this review acknowledge that drug design and discovery remains a team effort, involving the expertise of computational chemists, structural biologists, medicinal chemists, pharmacologists, toxicologists, clinicians, *etc.*

1) Captopril (Capoten®, Bristol Myers-Squibb)

Angiotensin-converting enzyme (ACE) is a carboxypeptidase with a zinc ion as a cofactor and plays a key role in the rennin-angiotensin cascade involving blood pressure control. The design of the antihypertensive drug captopril, a clinically important, potent and reversible inhibitor of ACE, is an example of one of the early endeavors and successes of structure-based drug design [1,2]. Information necessary for the design of captopril included knowledge that the enzymatic mechanism of ACE was similar to that of carboxypeptidase A, with an exception that ACE cleave off a dipeptide whereas the carboxypeptidase A cleave a single amino acid residue from the carboxyl end of protein. The discovery of L-benzylsuccinic acid **1** as a potent inhibitor of carboxypeptidase A [3] and studies of BPP5a (HOOC-Glu-Lys-Trp-Ala-Pro-NH), a potent pentapeptide inhibitor of ACE that was isolated from the venom of the Brazilian viper (*Bothrops jararaca*) [4], identified that N-terminal peptide fragments, including tetra, tri, and dipeptide fragments (Ala-Pro) retained inhibitory activity of the parent molecule. L-Benzylsuccinic acid **1** has been classified as byproduct-type of carboxypeptidase A inhibitor [3]. In design of this compound details of the two peptide fragments formed in the peptidase reaction, i.e. one with a free carboxyl end that coordinates with the zinc ion of the protease and another with a free amino terminus, were included. In the case of benzylsuccinic acid, the amino functionality is replaced by an isosteric methylene group. Using benzylsuccinic acid as a model compound, it was hypothesized that succinyl amino acids could also behave as byproduct inhibitors of ACE. Starting with a succinyl-proline **2** scaffold, structure-activity relationship (SAR) studies were critical in guiding the synthesis of captopril **4** (IC_{50} = 23 nM) [1,2]. Initially a stronger zinc-coordinating mercapto functionality replaced the carboxylic residue of succinic acid and a stereospecific *R*- methyl group was added to the succinyl moiety to emolate the methyl group that is naturally present in the L-Ala residue of Ala-Pro **3**. Captopril **4** pioneered by Cushman and Ondetti became the first ACE inhibitor to enter clinical use following its approval by the US FDA in 1981 and soon thereafter it established itself as a frontline therapeutic agent for the treatment of hypertension and heart failure.

2) Dorzolamide (Trusopt®, Merck)

An iterative approach as described above has been used to facilitate the optimization of carbonic anhydrase inhibitors with the goal of maximizing potency in a structural series having a proper balance between aqueous solubility and lipophilicity, which has permitted topical use in the treatment of the ocular disease, glaucoma. Inhibitors of this class should influence fluid dynamics in eye by blocking the local conversion of carbon dioxide to bicarbonate. This conversion is a critical step in the active secretion of aqueous humor, a fluid that fills the anterior and posterior chambers of the eye. The isozyme found within the secretory cell is carbonic anhydrase II (CA II) and it is this isozyme that has served as a structural model for understanding the inhibitory differences in the enzyme-ligand complexes for this target class [5]. The active-site cavity of human CA II (HCA II) is cone shaped and becomes very narrow at the catalytic hydrophobic pocket where zinc is coordinated in a tetrahedral fashion to three histidine residues: His94, His119, and His96. The active-site cavity is amphiphilic; one wall is dominated by hydrophobic and the other by hydrophilic residues [6-10].

The prototype compound **5** (MK-927), is a water soluble compound that rapidly penetrates ocular tissue, and lowers intraocular pressure (IOP) in animal models [5]. Chiral resolution generated two enantiomers, which differ in affinity by 100-fold, as measured in a competition assay versus dansyl amide. Both the *S*-enantiomer (more active) and *R*-enantiomer (less active) have been cocrystallized with HCA II [5]. Baldwin *et al.,* have used X-ray crystallographic data of the *S*- and *R*-enantiomer bound to HCA II to understand this 100-fold difference in affinity. They identified that the sulfonamide group in both enantiomers was coordinated to zinc within the catalytic site through the presumably deprotonated sulfonamide nitrogen while the thiophene ring was positioned between the hydrophobic and hydrophilic walls of the active-site cavity [6-10]. Both enantiomers placed the alkyl amino group in the less favored pseudo-axial orientation. *Ab initio* calculations at the 6-31 *G** level

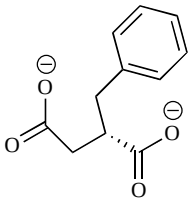

Benzylsuccinic acid
1

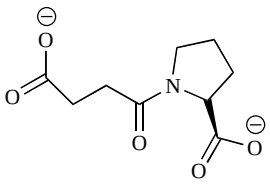

Succinyl proline
2

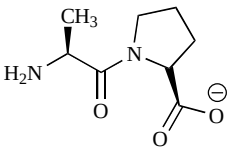

Ala-Pro
3

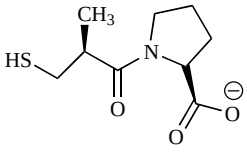

Captopril
4

suggested that the pseudoequatorial conformer would be preferred by about 1 kcal/mol.

The overall geometry of the two inhibitors was similar; however, two significant differences were noted between the enantiomers. First the N-S-C-S dihedral angle which was determined to be 150° for the *S*-enantiomer and 170° for the *R* represents a 20° twist of the thiophene ring in the *R*-isomer relative to the *S*. *Ab initio* molecular orbital calculations at the 3-21 *G** level supported that the preferred dihedral angle, which was calculated to be 72° implied that while the angle formed in the *S*-enantiomer is not ideal it is preferred by a ΔH of 1 kcal/mol. A second conformational difference between the two enantiomers involved the geometry of the 4-isobutylamino substituent. This side chain is *trans* in the *S*-enantiomer and *gauche* in the *R*. *Ab initio* calculations at the 3-21 *G** level suggest that the *trans* geometry should be preferred by 1 kcal/mol. The authors concluded that these two conformational features account for the 100-fold difference in affinity and potency that was observed experimentally for the two enantiomers [5].

Given that the isobutylamino group is oriented in the higher energy pseudo-axial conformation within the active-site cavity, it was hypothesized that further improvements in affinity could be achieved through reductions in this energetic penalty. In one such approach a methyl group was introduced into the 6-position of the thienothiopyran ring system; *ab initio* calculations inferred that this should eliminate the pseudoequatorial preference [5]. To counter the enhanced lipophilicity introduced by the methyl substituent, the 4-isobutylamino group was modified to an ethylamino moiety which resulted in the discovery of Dorzolamide **6** (Trusopt®, approved by FDA in 1994). All four possible optical isomers were prepared and cocrystallized with HCA II, and the structure for each complex was determined by X-ray crystallography [5,11]. The isomer with the greatest inhibitor potency and affinity had the trans *S,S* configuration and a K_i value of 0.37 nM. The structural information gained from X-ray crystallography established that the major conformational difference of the four optical isomers bound within the active site was the thiophenesulfonamide N-S-C-S dihedral angle. This torsion angle ranged from 140° for the *S,S*-isomer to 175° for the *R,R*-isomer [5,11].

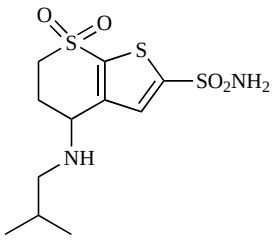

5 (MK-927)

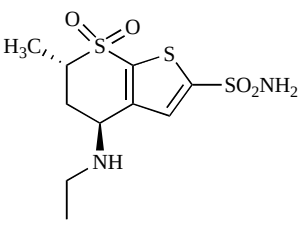

6 (Dorzolamide, Trusopt®)

X-ray crystallographic analysis indicated that the 6-methyl group was immediately above a lipophilic groove, one wall of which is formed by Phe131. In all of the examples studied by X-ray crystallography in this iterative approach, the side chain of His64 rotated 3.1 Å from its position in the native enzyme. Through further SAR and structural data, Baldwin *et al.* [5] and Greer *et al.* [11] established that the rotation of His64 side chain was the result of a 4-alkylamino substituent.

3) Saquinavir (Invirase®, Hoffmann-La Roche)

Inactivation of the human immunodeficiency virus-1 protease (HIV-1 PR) by either mutation or chemical inhibition results in the production of immature, noninfectious viral particles [12-14]. On the premise that PR represents an essential proper virion assembly and maturation, HIV-1 PR became an important target for the design of anti-HIV drugs. Not surprisingly, since 1995 several such drugs have been developed through transition-state mimetics [13,15] and structure-based synthetic strategies, and have received federal approvals for use in the United States [16]. For example, Saquinavir (Invirase®, Hoffmann-La Roche), approved in 1995 is the first example of a HIV-1 protease inhibitor with clinical utility (IC_{50} = 0.4 nM), hence, it is the only example discussed here in the interest of saving space. This compound was designed on the basis of Phe-Pro substrates which, until the late 1980s were known to be cleaved by HIV-1 PR but not by mammalian proteases, a feature that promised selectivity toward its target [17]. Crystallographic study of the complex between the peptidic inhibitor **7** (Ro 31-8558) and HIV-1 PR showed the expected mode of binding and at the same time suggested possible future modifications [18]. Further structure-based optimization of **7** resulted in compound **8** (Ro 31-8959) [17], later designated saquinavir, which is a pentapeptide derivative featuring an hydroxylethylamine transition state moiety in place of the cleavable peptide bond, a bulky (*S,S,S*)-decahydro-isoquinolin-3-carbonyl (DIQ) group in place of proline at P1′ and a quinoline at P3. X-ray determination of the co-crystal structure complex of saquinavir and HIV-1 PR revealed that the carbonyl group of DIQ moiety is able to form a hydrogen bond with the water molecule connecting the inhibitor with the flap regions [19]. Saquinavir inhibits one of the last stages of viral replication, and is found to be active in cell culture against both HIV-1 and HIV-2 viruses (EC_{50} ~ 1–30 nM).

4) Zanamivir (Relenza®, Gilead Sciences)

Neuraminidase (NA) enzymes, also known as sialidases are phylogenetically categorized into two groups: group-1 includes N1, N4, N5, and N8 and group-2 includes N2, N3, N6, N7, and N9 [20], are an essential components of the influenza virus envelope that is involved in the hydrolytic cleavage of glycosidic bonds between terminal sialic acid residues and adjacent sugars on hemagglutinin and/or on the surface of host cells [21,22]. The cleavage of the sialic acid bond (α 2,3 or α 2,6 linkage) facilitates the spread of the virus by promoting the release of progeny viral particles from infected host cells and, thus the infection of new host cells [23]. The determination of the 3D structure of group-2 neuraminidase in 1983 enabled the structure-based design of active anti-influenza viral agents that were developed around the highly conserved structure of the active site [24]. In an elegant study, von Itzstein *et al.*, [25] investigated the binding site of neuraminidase and determined interaction energies through the use of different probes and the computer program GRID [26]. Neuraminidase inhibitors

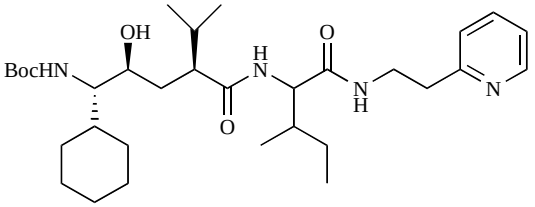

7 (Ro 31-8558)

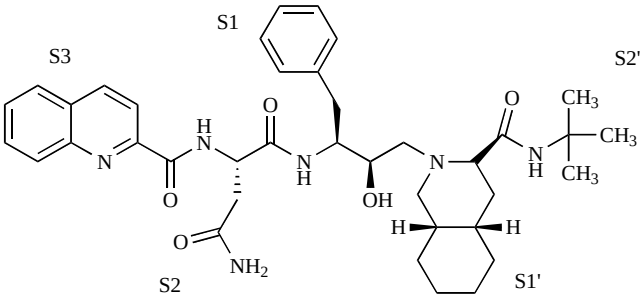

8 (Saquinavir, Ro 31-8959

were designed following a similar "transition-state" principle [27] as applied for the discovery of peptidomimetic HIV-1 PR inhibitors (e.g., Saquinavir) as discussed above.

The receptor site to which the sialic acid portion of the virus binds was defined by crystallographic studies of 2-deoxy-2,3-dehydro-*N*-acetylneuraminic acid (DANA) **9** bound to neuraminidase [28]. These studies proposed that substitution of the 4-hydroxy moiety with an amino group or the larger guanidine group should improve the binding of the inhibitor to neuraminidase active site [28]. The 4-amino derivative was found to bind to Glu119 in the receptor through a salt bridge, whereas the guanidino group was able to form both a salt bridge to Glu119 and a charge-charge interaction with Glu227 [25]. These substitutions resulted in a dramatic increase in binding to neuraminidase, which translated into the development of potent competitive inhibition of the enzyme [29]. This compound, designated as Zanamivir (Relenza®) **10**, is a first-in-class neuraminidase inhibitor that received US FDA approval in 1999 for the treatment of the influenza A and B viruses. Zanamivir is administered through inhalation because of its poor oral bioavailability [30]. The discovery of Zanamivir demonstrated the power of rational, structure-based and computer-assisted drug design and provided a platform for further neuraminidase-targeted antiinfluenza drugs [31].

However, since the oral route is more convenient and economical for treatment and prophylaxis of patients diagnosed with the influenza virus especially during an epidemic, it was realized that a potent neuraminidase inhibitor that is bioavailable would be ideal. With this goal, investigators at Gilead Sciences designed transition-state analogs of sialic acid [31]. The design strategy was based on utilizing a more chemically stable carbocyclic core rather than the dihydropyran core as a mimic of the planar oxocarbonium intermediate [31]. X-Ray crystallographic studies have further demonstrated that additional binding sites exist between neuraminidase and its substrate (sialic acid) that involves interactions between the C-5 acetamido carbonyl and Arg152; the C-2 carboxyl and residues Arg118, Arg292, and Arg371; and the potential for hydrophobic binding between the substituents at the C-6 position and hydrophobic residues that include Ile222 and Ala246 [31]. SAR exploration based on these findings eventually led to the development of oseltamivir (GS4071) **11**. Oseltamivir (Tamiflu®, Gilead Sciences) is a prodrug which undergoes hepatic hydrolysis to an active carboxylic acid. Oseltamivir (approved by the US FDA in late 1999) was the first commercially available oral neuraminidase inhibitor with activity against both influenza A and B viruses. This is a front line agent that is currently being used to treat our current world wide outbreak/epidemic of swine flu (H1N1) along with Zanamivir (Relenza®) discussed above.

5) Aliskiren (Tekturna®, Novartis)

The renin-angiotensin system (RAS) is a key regulator of blood pressure and body fluid volume through a mechanism that involves the octapeptide hormone, angiotensin II (Ang II). Ang II is formed in a two-step process: the aspartic peptidase renin cleaves the Leu10-Val11 peptide bond of angiotensinogen to form angiotensin I (Ang I), which is then converted by angiotensin converting enzyme (ACE) into Ang II. Thus, renin is an attractive target for rational drug design for the treatment of hypertension [32]. To this end, the combined application of crystallographic structure studies of renin-inhibitor complexes with computational approaches have guided the design and synthesis of several novel, low molecular weight, renin inhibitors that lack the extended peptide-like backbone of earlier generation inhibitors and have more favorable pharmacokinetic (PK) properties that enable oral administration [33].

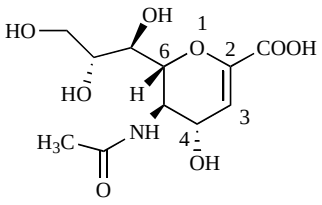

DANA
9

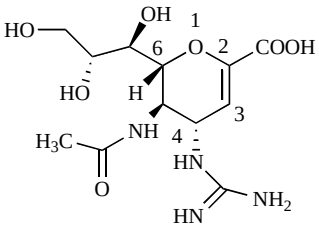

Zanamivir
10

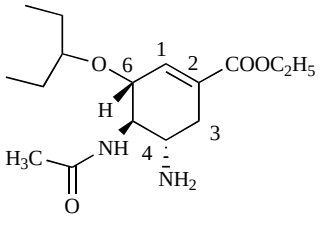

Oseltamivir
11

The developmental history of aliskiren can be traced back to first generation peptide-like renin inhibitors such as **12** (CGP29287), which is related to the structure of the natural substrate of the renin system which exploits the so-called 'transition state theory' [34]. CGP38560 (**13**) is a second generation peptide-like renin inhibitor that was a clinical disappointment because of a low oral absorption and a rapid biliary excretion [35,36]. Given this and other failures in this target space the development of novel renin inhibitors was transformed when Goschke *et al.,* [37] recognized that non-peptidic analogs might be better suited for overcoming the difficulties (poor oral bioavailability, limited plasma pharmacokinetic properties and low specificity) associated with peptidic compounds.

Molecular modeling methods were used to design compounds lacking the P1–P4 backbone-like architecture of first- and second-generation peptide inhibitors that allowed Goschke *et al.,* [37] to exploit the extended hydrophobic surface of the large S3–S1 cavity of renin. This design approach utilized a dipeptide-like hydroxyethylene transition state mimetic with a directly linked P3–P1 pharmacophore, resulting in the synthesis of the novel lead compound **14** [37]. This lead compound inhibited purified recombinant human renin at nanomolar concentrations but its activity was reduced in the presence of plasma [33]. Computational modeling partnered with structural details provided by X-ray crystallographic resolution of enzyme–inhibitor complex guided further optimization of this lead compound with the aim of improving its potency when tested in the more physiologically relevant plasma renin assay [33].

The tertiary butyl and methyl acetoxy groups on the aromatic ring in the lead compound **14** were replaced by the smaller polar -OCH_3 and alkylether substituents respectively to provide nanomolar renin inhibitors [37]. Furthermore, X-ray structure analysis showed that these compounds interacted with a distinct subpocket, S3, oriented perpendicularly to the substrate binding cleft of renin, which is not occupied by substrate-derived peptide-like inhibitors including compound **13** [35]. Exploitation of this previously unrecognized site, mostly through optimization of the hydrophobic interactions within the S3 subpocket, dramatically enhanced both the binding affinity of renin and selectivity over related aspartic peptidases [38]. A journey from lead compound **14** to Aliskiren **15** (SPP-100) required the synthesis of several potent renin inhibitors [33,36-38]. A structure-based analysis of these compounds allowed Cohen and Wood group to conclude that the methoxypropoxy side chain was optimal in terms of its length and the position of its distal ether oxygen, which serves as a H-bond acceptor from Tyr14 of the S3 subpocket. At the P1′ position, substitution of the methyl group for an isopropyl moiety coupled with extensive modifications of the P2′ portion, including replacement of the n-butyl side chain with a terminal carboxamide group, created an additional H-bonding interaction with Arg74. Furthermore, the insertion of a geminal methyl moiety into the P2′ side chain provided hydrophobic van der Waals interactions with the S2′ site of renin [33]. As a result of all these structure/function modifications, compound **15**, which is referred to as Aliskiren (Tekturna®, Novartis) has a demonstrable inhibitory potency for renin that is in the sub-nanomolar range evolved. As a hemifumarate salt, this small molecule, non-peptide transition-state mimetic, human renin inhibitor received FDA approval in 2007 [36].

6) Boceprevir (Schering-Plough)

Given the established role for the NS3-NS4A serine protease in hepatitis C virus (HCV) replication, it is an ideal target for the development of new anti-HCV therapy [39,40]. At the onset of this work, no viable lead structures from which one could develop potential drug candidates against HCV existed. The failure of HTS efforts to identify potential lead compounds for initiating a drug discovery effort in this space forced a team of scientists from Schering-Plough Research Institute to commence a structure-based design approach [41]. Early research on first generation NS3-NS4A protease inhibitors capitalized on the observation that this enzyme is markedly inhibited by N-terminal peptide products that are released following enzymatic cleavage of native substrates. Others have demonstrated that numerous potent, serine-protease inhibitors [42] incorporate a serine trap into their architecture and thus it was rationalized that Ser139, which is within the active site of the viral protease [43] may react with conventional electrophiles such as aldehydes, ketones, trifluoromethyl ketones, and α-keto-amides. It was hypothesized that trapping the resulting transition-state analogues through an active site amino acid triad Ser139, His57, and Asp81 [43] would provide effective inhibition.

Early work at Schering-Plough Research Institute led to the discovery of series of undecapeptide α-ketoamide inhibitors [44], whose structures are comprised of amino acid residues that span from P6 to P5′ [45]. One of the earliest leads, compound **16**, exhibited excellent anti-HCV NS3-NS4A protease activity (K_i^* = 1.9 nM, K_i* represents binding for a mixture of diastereomers at P1). A lead optimization program involving X-ray structures of compound **16** and related analog inhibitors bound to the HCV NS3 protease was established that resulted in identification of compound **17** with K_i^* of 25 nM, and a replicon EC_{90} of 0.4 μM [41].

Extensive SAR investigations around the P1, P3, and P3-capping positions of the lead compound **17** was carried out. Since the dimethylcyclopropylproline moiety at the P2 position was found to be optimal, it was retained in the structure of all subsequent analogs. Systematic variation in chain length and ring size on the P1 side chain led to the discovery of cyclobutylalanine as the optimal choice [41]. Among several P3 capping groups explored, the urea type of P3 cap gave the best overall profile. Eventually, the combination of various optimized moieties led to the discovery of compound Boceprevir (SCH503034) **18** [44], which has a K_i^* = 14 nM, EC_{90} = 0.35 μM [41]. Recently, Njoroge *et al.,* [41] have written a case study of Boceprevir, which is currently in a phase III clinical trials.

7) Nolatrexed dihydrochloride (Thymitaq®, Agouron)

As part of a research program aimed at developing new anti-cancer chemotherapeutics, Dr. Webber and his group at Agouron Pharmaceuticals considered the enzyme thymidylate synthase (TS) as a biochemical target for drug design [46]. This enzyme catalyzes the conversion of deoxyuridine

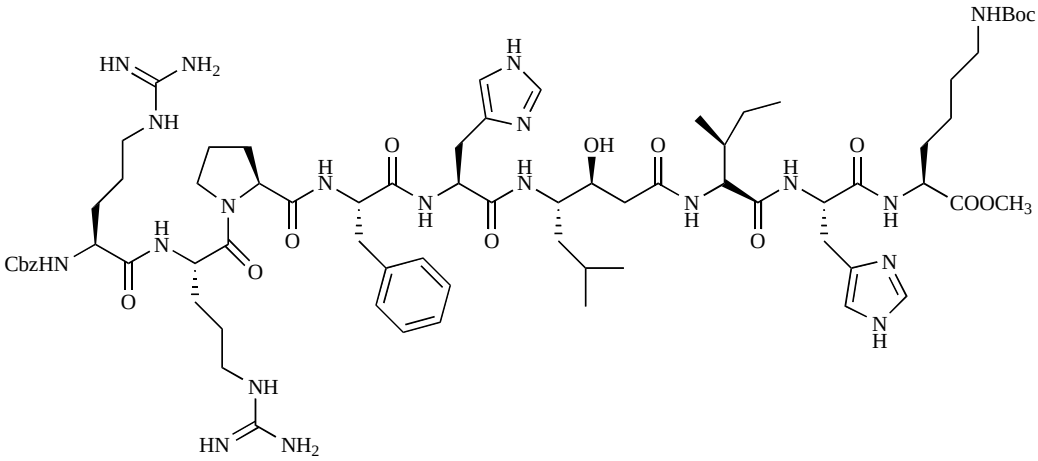

First generation Renin inhibitor: **12**, CGP29287

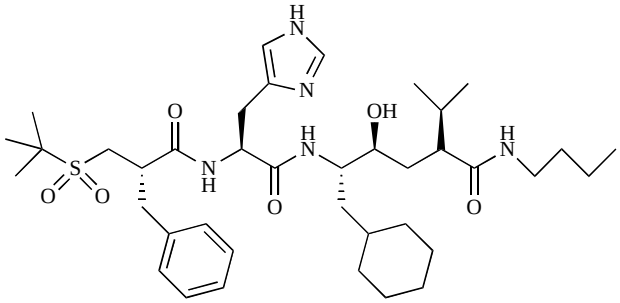

Second generation Renin inhibitor: **13**, CGP38560

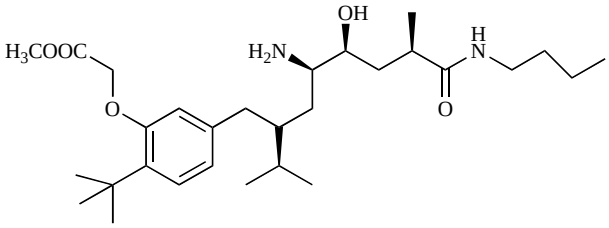

Third generation Renin inhibitor: Lead compound **14**

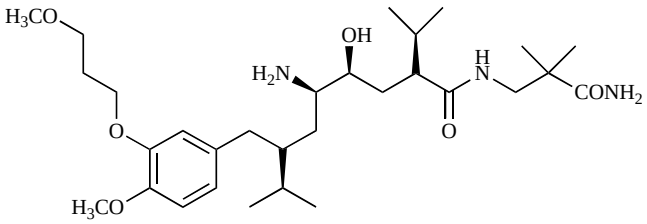

Third generation Renin inhibitor: **15**, Aliskiren (Tekturna(R))

monophosphate (dUMP) to deoxythymidylate (dTMP) through a reductive methylation step that uses 5,10-methylenetetrahydrofolate as a cofactor. The rate-limiting step of this conversion is the *de novo* source of dTMP for DNA biosynthesis. In the absence of exogenous source of thymidine, TS activity will cease and a "thymineless cell death" will ensue [46].

Initial drug design work on TS inhibitors involved high-resolution X-ray crystal structure data and structure-based molecular modeling methods, which led to the synthesis of four different quinazolinones [46], each substituted at the C-5 position. Among these derivatives, compound **19** (CB3717) [47] was found to exhibit measurable inhibitory activity against human and *Escherichia coli* TS. The

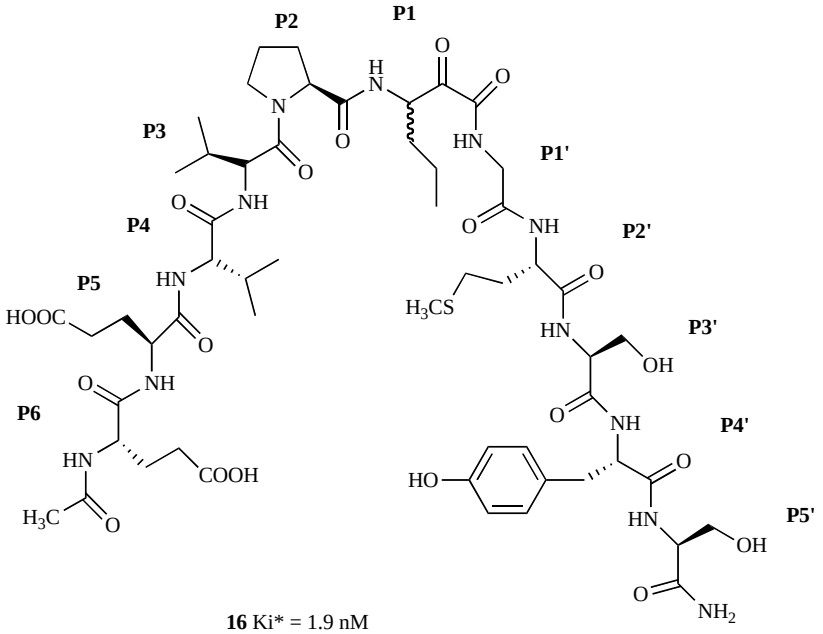

16 Ki* = 1.9 nM

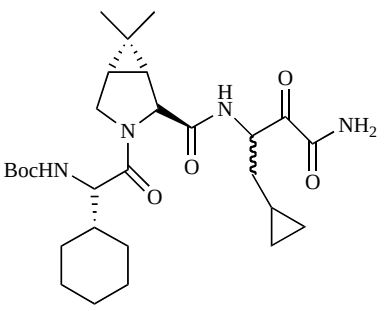

17 Ki* = 25 nM; EC_{50} = 0.4 μM

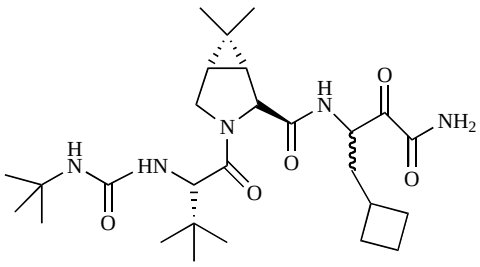

18 Ki* = 14 nM; EC_{90} = 0.35 μM

Ki* value represents binding for a mixture of diasteromers at P1

enzyme-ligand crystal structure of TS bound to compound **19** was solved and utilized for subsequent design [48].

At the onset of work aimed at designing TS inhibitors the structure of human TS was not available and thus the bulk of the research in this area was carried out using *E. coli* TS. With the exception of the three residues His51, Trp83, and Val262 (Phe80, Asn112, and Met311; human nomenclature) the folate binding site of the *E. coli* and human TS enzyme are homologous. Given this similarity initial structure-based drug design strategies involved the ternary complex of *E. coli* TS, 5-FdUMP and compound **19** (CB3717), which was resolved at 2.3 Å [48]. The quinazolin-4-one ring was kept intact as this ring was involved in important hydrogen bonding interactions with the active site residues as well as aromatic pi-stacking interactions. The 2-amino group on the quinazolinone nucleus was replaced with 2-methyl for the sake of initial synthetic ease. The design strategy was mainly focused on C5-C6-C9 and *para*-aminobenzoyl regions of **19**.

Upon closer inspection of the binding conformation of **19** as well as models of 5,10-methylenetetrahydrofolate, it became apparent that the hydrophobic cavity associated with the *para*-aminobenzoyl portion of these structures could be accessed from C-5 and N-5, respectively [46]. A one-atom linkage between the phenyl or aromatic ring and C-5 of the quinazolinone system was envisaged. Based on this general idea, four different quinazolinones, each substituted at the C-5 position were synthesized. Among these derivatives, the pyridine derivative **20** exhibited measurable inhibition constants of 10.0 μM against *E. coli* and 0.96 μM against human TS. The ternary crystal structure complex of *E. coli* TS, 5-FdUMP and compound **20** facilitated further design strategies for next generation compounds with a focus on binding to the C-6-Trp80 region of the enzyme-ligand complexes [46]. However, since C-6 of compound **20** is unsubstituted when compared with compound **19**, in which a methylene moiety occupies the space and is in hydrophobic interaction with Trp80, a methyl group was introduced at C-6 position of **20** to get compound **21**, which when docked into the active site, the C-6 methyl group filled the empty gap efficiently and contributed to improved affinity for *E. coli* (0.50 μM) and human TS (0.093 μM) than previously observed for other compounds in this series [46].

Inspection of the ternary crystal complex of **21** supported that replacing the quinazoline C-2 methyl by an amino group introduced a hydrogen bond involving the backbone carbo-

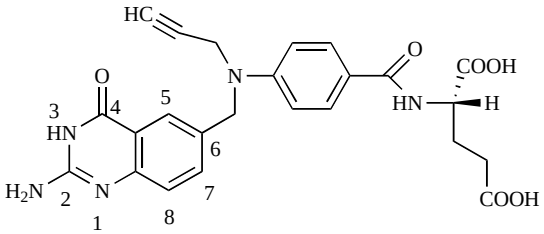

19 (CB3717)

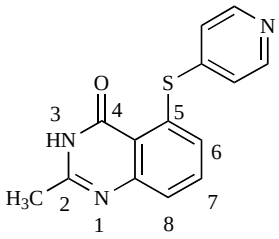

20

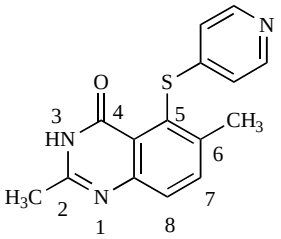

21

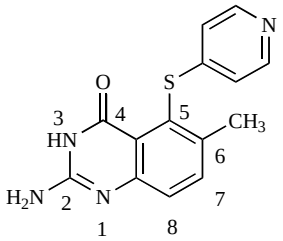

22 (Nolatrexed, AG337)

nyl oxygen atom of Ala263 [46]. Subsequently, Nolatrexed (AG337, Thymitaq®, Agouron) **22** was synthesized and shown to be more potent at inhibiting *E. coli* TS (49 nM) and against human TS (15 nM), (10- and 6-times) respectively, than compound **21** [46]. Currently, Nolatrexed is in a phase III clinical trial for the treatment of liver cancer.

8) TMI-005

Tumor necrosis factor-α converting enzyme (TNF-α convertase, TACE) is a zinc metalloenzyme that mediates the hydrolysis of a Ala-Val bond of the membrane-bound, 26 kDa pro-TNF-α resulting in the release of TNF-α, a soluble immunoregulating cytokine into the circulation [49]. TNF-α is a major proinflammatory mediator that is overproduced in inflammatory diseases such as rheumatoid arthritis, multiple sclerosis, diabetes, ulcerative colitis and Crohn's disease, and in congestive heart failure [50]. As a result inhibition of TACE is an attractive treatment strategy for patients diagnosed with these debilitating diseases. Drugs that manage these inflammatory diseases by reducing the levels of TNF-α provide a strategy to manage cytokine levels. Analysis of X-ray co-crystal structure data suggested rational modifications of early sulfonamide hydroxamate TACE inhibitors (compounds **23** and **24**) could improve potency and selectivity over matrix metalloproteases (MMPs) [51]. The S1′ pocket of TACE consists of an initial region that resembles the shallow S1′ pocket of MMP-1 in size and depth. The rest of the TACE S1′ is not extended linearly as is the case with MMP-9 and MMP-13; rather, it is present as an extended channel which is almost perpendicular to the S1′ pocket and directed toward the S3′ surface [51]. Based on these observations, a solid phase combinatorial chemistry approach was used to generate a library of phenoxyacetylene hydroxamates [52]. Optimization of these leads for potency and selectivity helped to define SAR requirements for the TACE binding site [52]. Subsequent optimization for PK activity and *in vivo* efficacy through parallel synthesis led to the discovery of compound **25** (TMI-005), a propargylic hydroxylhydroxyamic acid that is being evaluated in phase II clinical trial for the treatment of rheumatoid arthritis [53].

9) LY-517717 (Lilly/Protherics)

Researchers at Protherics used library design and structure-based virtual screening to develop inhibitors of factor Xa serine protease, an important target in the blood coagulation cascade [54]. Using a rational approach commencing with the known benzamidine inhibitor fragment **26** that has a well defined interaction mode as determined in X-ray crystallographic studies an iterative library design was used to identify a number of lead molecules including amidine **27** [54]. Amidine-containing compounds were shown to have antithrombotic activity but poor oral bioavailabilty, presumably because of the presence of the basic benzamidine moiety, which is known to hinder absorption from the gastrointestinal tract. Hence, replacing the benzamidine moiety with an uncharged indole, which retains favorable interactions with a catalytic aspartate residue gave rise to compound **28** (LY-517717), exhibiting K_i = 0.005 μM and good oral pharmacokinetic properties [55]. Discovery of compound **28** is an example of application of classical medicinal chemistry facilitated by structure-based drug design. Compound **28** (LY-517717) is currently under phase II clinical development for the prevention of venous thromboembolism after hip or knee replacement [56].

10) Rupintrivir (AG7088, Agouron)

Human rhinovirus (HRV) 3C protease is a viral enzyme which catalyzes the cleavage of host cell translated viral polyproteins into functional structural and enzyme proteins required for the replication of the virus responsible for the common cold and other infections of the upper respiratory tract [57]. This protease belongs to a unique class of enzymes that integrate the characteristics of both serine and cysteine proteases with an unusual specificity for Gln-Gly cleavage junctions [58]. The availability of a recombinant 3C protease has facilitated a better understanding of bio-

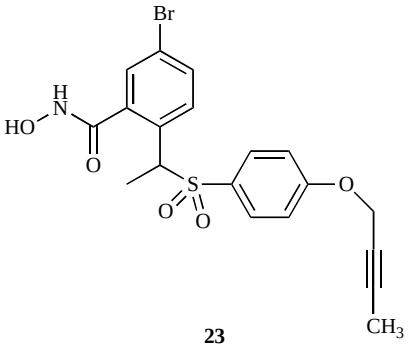

23

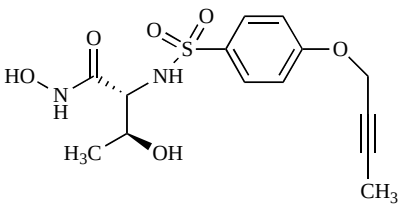

24

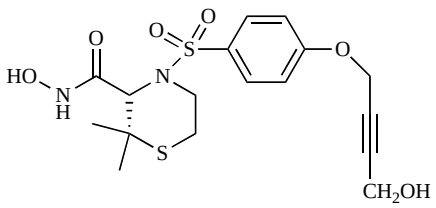

25 (TMI-005)

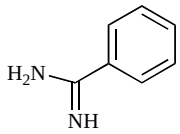

26 Ki = 200 μM

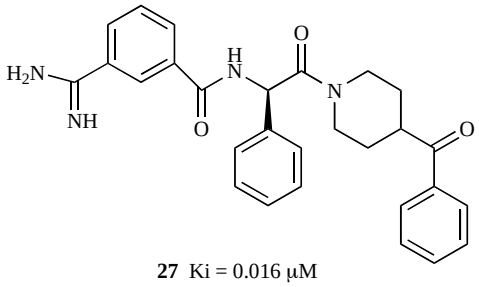

27 Ki = 0.016 μM

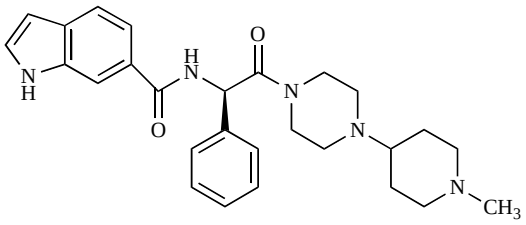

28 (LY-517717) Ki = 0.005 μM

chemical properties of this enzyme. The absence of known cellular homologues have contributed to the present interest of the 3C protease as a potential target for antiviral drugs able to control HRVs and the common cold. Early inhibitors of 3C proteases were based on the structure of peptide aldehyde inhibitors of serine and cysteine proteases [59-61]. Early studies demonstrated that the aldehydic carbonyl carbon can covalently and reversibly bind to the nucleophilic cysteine (Cys147 in 3C proteases) or serine (from serine proteases) residues of the active site to form a stable tetrahedral species. However, the interaction of the glutamine at P1 with the aldehyde functionality may cause cyclization on the aldehyde [62]. This problem has been circumvented by substituting a γ-carboxamide moiety for the aldehyde group, which removes this potential without a loss of the high affinity for the 3C protease S1 specificity pocket [61]. Compound **29** is an N-terminal protected tripeptide aldehyde in which the $-CH_2C(=O)NH_2$ of Gln has been replaced by an *N*-acetyl isostere. As such, compound **29** is a potent (K_i = 6 nM) inhibitor of type 14 rhinovirus 3C protease [63,64]. Further structure-based lead optimization studies were facilitated by determining the X-ray crystal structure of serotype 2 rhinovirus 3C protease-compound **29** complex [61]. The X-ray structure analysis of 3C proteases from several serotypes suggested that residues 69 (Lys or Asn, depending on the serotype) and 130 (Asn or Thr) that are located at the back of the S2 specificity pocket are not conserved with their side chains interacting with compound **29** [63]. Thus, the available crystallographic and amino acid sequence data suggest that inhibitors of rhinovirus 3C protease would be expected as active against the enzyme from multiple viral serotypes provided that they do not depend on binding determinants at the back of the S2 specificity pocket where structural variability between serotypes may be most pronounced.

Extensive SAR studies directed at optimizing the Michael acceptor group led to the identification of *trans*-α,β-unsaturated esters as the Michael acceptors of choice around which Dragovich *et al.,* [64] initiated a peptidomimetic optimization strategy around compound **30** [65]. Further structure-based SAR investigations were conducted with tripeptide-derived molecules at P1, P2, P3 and P4 side chains, which ultimately resulted in identification of **31**, commonly known as Rupintrivir (AG7088) [64].

Co-crystal structure of 3C protease of serotype 2 with compound **30** indicated that the P1 side-chain *cis*-NH is exposed to solvent and, as a result, the terminal amide group could be modified to reduce the peptide character of the inhibitor without compromising its binding ability. Structure-based molecular modeling studies further led to the incorporation of the P1 lactam moiety with (*S*) stereochemistry at its α-carbon so that it would be correctly positioned into the S1 pocket. The resulting molecule was 10-fold more potent than compound **30** against type 14 3C protease and more than 5-fold better as an antiviral agent in a cell culture assay [66].

Co-crystal structure of 3C protease in complex with compound **30** suggested that the S2 specificity pocket is large and could accommodate substituents at the *para*-position of the P2 side chain. This observation led to the *para*-fluoroPhe analog which exhibited a modestly better potency than the parent compound in *in vitro* assays against 3C protease from serotypes 2, 14, and 16 [64]. The P2 backbone amide of compound **30** donates a hydrogen bond to the side-chain oxygen of invariant Ser128 located in a conformationally flexible and somewhat solvent-exposed loop forming one side of the S2 specificity pocket. These findings were later translated into replacement of the P2–P3 peptide bond with a ketomethylene functionality to reduce the peptidic character of the resulting molecule, with the

hypothesis that loss of the exposed surface hydrogen bond may not impact inhibitory activity. Although the keto-methylene inhibitor showed slightly reduced 3C protease inhibition when compared to compound **30**, however it demonstrated improved antiviral properties [67].

The leucine side chain of compound **30** being solvent-exposed can accommodate a wide variety of functionalities without impacting appreciably on its enzyme inhibitory activity. This observation resulted in replacement of the leucine side chain with that of valine at the P3 position [64].

Finally optimization of the carbobenzyloxy (Cbz) group at the P4 position of the tripeptidyl ethyl propenoate Michael acceptor of the sequence Leu-Phe-Gln was carried out by reacting the N-terminal amine group with variety of carboxylic acids and acid chlorides to generate approximately five hundred different N-terminal protected tripeptide Michael acceptors. Among these products, the N-terminal 5-methyl-isoxazole-3-carboxamide analog was identified as a potent 3C protease inhibitor with improved antiviral activity (EC_{50} = 0.25 μM) compared with that of compound **30** [68].

A SAR investigation that took into consideration the optimum P1-P4 groups in compound **30** led to discovery of the 3C protease inhibitor **31** (AG7088, Rupintrivir), a potent antiviral agent against multiple serotypes of HRV [69]. Despite of some success in phase II/III trials in patients that were experimentally infected with HRV, Rupintrivir was not able to mitigate disease severity in studies of natural rhinovirus infection, hence, further clinical development was stopped on the basis of this missed end point [70].

11) NVP-AUY922 (Novartis)

The molecular chaperone heat shock protein 90 (HSP90) supports the correct conformation, stabilization, activation, and localization of ''client'' proteins, many of which are involved in tumor progression, hence HSP90 is an ideal and novel target in cancer therapy [71-74]. This 90 kDa chaperone hydrolyses ATP as part of its biochemical actions. The structure and functions of HSP90 have been elucidated in considerable detail, particularly with the aid of X-ray crystallography [74]. HSP90 is made up of three functional domains: an NH_2-terminal ATP/ADP-binding domain, a middle domain involved in client protein binding, and a COOH-terminal dimerization domain [74].

High-throughput screening experiments resulted in the small molecular size pyrazole resorcinol inhibitor **32** (CCT018159) [75-77]. Subsequent co-crystal structure complex of HSP90-compound **32** suggested structural sites where additional atoms could be placed to increase the binding of the drug to the protein, and where space was available for adding groups to improve pharmacokinetic properties. Medicinal chemists from The Institute and Vernalis Ltd. have applied iterative structure-based design for the optimization of **32**. Key steps on the way from CCT018159 through VER-49009 **33** [78] and VER-50589 **34** [79] to NVP-AUY922 **35** [80] were the addition of an amide group to improve binding to the protein, as in **33**, and the correct placement of a group to improve solubility and pharmacokinetic properties. Modification of the pyrazole by the addition of other chemical groups capable of maintaining interactions with HSP90 shown by X-ray crystallography led to a series of isoxazoles, like compounds **34** and **35**, exhibiting potent activity in animal models of cancer. Following safety and toxicological studies, in collaboration with Novartis, NVP-AUY922 entered Phase I clinical trials in 2007 [81,82].

CLOSING REMARKS AND FUTURE OUTLOOK

Throughout this review we have used very specific examples extracted from the volumes of documented scien-

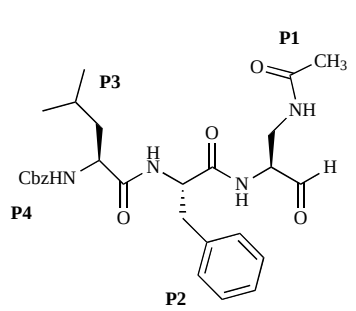

29

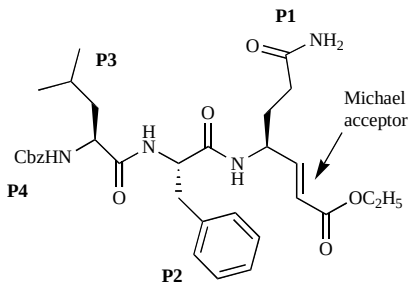

30

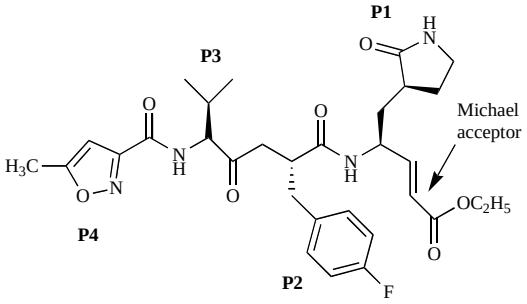

31, Rupintrivir (AG7088)

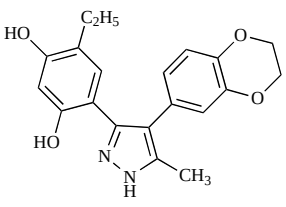

CCT018159
32

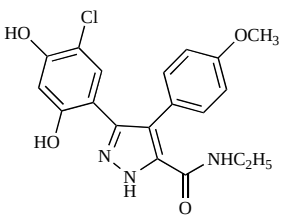

VER-49009
33

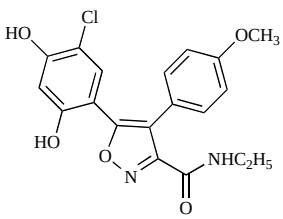

VER-50589
34

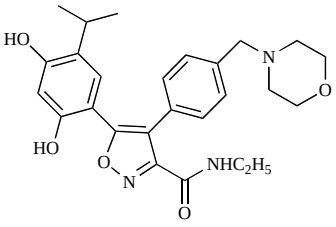

NVP-AUY922
VER-52296
35

tific literature in an attempt to articulate just how the iterative process of structure-based design, that partners the atomic details provided by experimental (X-ray) structures with computational structure-based design supported by medicinal chemistry strategies, can lead to the development of drugs or drug-like molecules with refined pharmacological activity that is better than the parent molecule. In recent years, structure-based drug design has been recognized as the tool that facilitated the development of several important drugs in current clinical use or late stage clinical development. Agouron and Vertex are two small biotechnology companies that have clearly documented the success of such an approach. Given the success of these and other small companies in this space many of the large pharmaceutical companies have shifted away from the more traditional, capital intensive HTS platform approach to a more targeted platform that leverages the power and speed of structure-based and/or computational-based approaches.

With the development of significantly more sophisticated molecular modeling tools and a growth in the use of high throughput X-ray crystallography of the target alone or in complex with small molecules, structure-based drug design techniques have become an indispensable tool for the development of target-based therapies. Importantly, these newly appreciated approaches are being supported and/or driven by rapidly improving computational platforms that are more reproducibly docking, scoring and ranking drug-like compounds, which has allowed many drug discovery scientists to carry out more focused, hypothesis-driven discovery initiatives limiting the number of compounds that are synthesized. It is important to note that the adoption of early stage PK and PD studies has also contributed greatly to the significantly reduced late-stage attrition rate of clinical candidates. In the particular case of drugs acting as inhibitors of specific target proteins, these advances together with a more careful attention to the conformation, mechanism of action, and drug-like property of the inhibitor are expected to result in novel therapeutic agents that are more potent, selective and bioavailable, which one can imagine should improve the probability that compounds developed using this iterative approach will meet their final end point, clinical validation.

ACKNOWLEDGEMENT

The author wish to thank Dr. Cesar A. Lau-Cam for critical readings of the review and for helpful discussions.

ABBREVIATIONS

ACE	=	Angiotensin converting enzyme
ADMET	=	Absorption, distribution, metabolism, excretion, toxicity
ADP	=	Adenosine diphosphate
Ang I	=	angiotensin I
Ang II	=	angiotensin II
ATP	=	Adenosine triphosphate
DANA	=	2-deoxy-2,3-dehydro-*N*-acetylneuraminic acid
DIQ	=	Decahydro-isoquinolin-3-carbonyl
dTMP	=	deoxythymidine monophosphate
dUMP	=	deoxyuridine monophosphate
EC_{50}	=	Effective concentration of an inhibitor with 50% inhibition of viral replication
HCV	=	Hepatitis C virus
HIV-1 PR	=	Human immunodeficiency virus
HRV	=	Human rhinovirus
HSP	=	Heat shock protein
HTD	=	High throughput docking
HTS	=	High-throughput screening
IC_{50}	=	Inhibitor concentration exhibiting 50% suppression of enzyme activity
K_i*	=	inhibition constant representing binding for a mixture of diastereomers (in this case at P1)
LBVS	=	Ligand-based virtual screening
MMP	=	Matrix metalloprotease
NMR	=	Nuclear magnetic resonance
PD	=	Pharmacodynamic
PK	=	Pharmacokinetic
RAS	=	Renin angiotensin system
SAR	=	Structure-activity relationship
SBVS	=	Structure-based virtual screening
TACE	=	Tumor necrosis factor-alpha converting enzyme
TNF-alpha	=	Tumor necrosis factor-alpha
TS	=	Thymidylate synthase

REFERENCES

[1] Cushman, D.W.; Cheung, H.S.; Sbo, E.F.; Ondetti, M.A. Design of potent competitive inhibitors of angiotensin converting enzyme. Carboxyalkanoyl and mercaptoalkanoyl amino acids. *Biochemistry*, **1977**, *16*, 5484-5491.

[2] Ondetti, M.A.; Rubin, B.; Cushman, D.W. Design of specific inhibitors of angiotensin-converting enzyme: new class of orally active antihypertensive agents. *Science*, **1977**, *196*, 441-444.

[3] Byers, L.D.; Wolfenden, R. Binding of the by-product analog benzylsuccinic acid by carboxypeptidase A. *Biochemistry*, **1973**, *12*, 2070-2078.

[4] Ferreira, S.H.; Bartelt, D.C.; Greene, L.J. Isolation of bradykinin-potentiating peptides from *Bothrops jararaca* venom. *Biochemistry*, **1970**, *9*, 2583-2593.

[5] Baldwin, J.J.; Ponticello, G.S.; Anderson, P.S.; Christy, M.E.; Murcko. M.A.: Randall, W.C.; Schwam. H.; Sugrue, M.F.; Springer. J.P.; Gautheron, P.; Grove, J.; Mallorga, P.; Viader, M.P.; McKeever, B.M.; Navia, M.A. Thienothiopyran-2-sulfonamides: novel topically active carbonic anhydrase inhibitors for the treatment of glaucoma. *J. Med. Chem.*, **1989**, *32*, 2510-2513.

[6] Erikeson, A.E.; Jones, T.A.; Liljas, A. Refined structure of human carbonic anhydrase II at 2.0 Å resolution. *Proteins*, **1988**, *4*, 274-282.

[7] Coleman, J.E. Chemical reactions of sulfonamides with carbonic anhydrase. *Annu. Rev. Pharmacol.*, **1976**, *15*, 221-242.

[8] Lindskog, S. The structural basis of kinetic differences between carbonic anhydrase isoenzymes. In: *Progress in Inorganic*

Biochemistry and Biophysics. Zinc Enzymes: Bertini, I., Luchinat, C., Marei, W., Zepkzauer, M., Eds.; Birkhauser Boston, Inc.: New York, **1986**, . *1*, 307-316.

[9] Silverman, D.N.; Lindskog, S. The catalytic mechanism of carbonic anhydrase: implications of a rate-limiting protolysis of water. *Acc. Chem. Res.*, **1988**, *21*, 30-36.

[10] Christianson, D.W. Structural biology of zinc. *Adv. Protein Chem.*, **1991**, *42*, 281-355.

[11] Greer, J.; Erickson, J.W.; Baldwin, J.J.; Varney, M.D. Application of the three-dimensional structures of protein target molecules in structure-based drug design. *J. Med. Chem.*, **1994**, *37*, 1035-1054.

[12] Kohl, N.E.; Emini, E.A.; Schleif, W.A.; Davis, L.J.; Heimbach, J.C.; Dixon, R.A.; Scolnick, E.M.; Sigal, I.S. Active human immunodeficiency virus protease is required for viral infectivity. *Proc. Natl. Acad. Sci. USA*, **1988**, *85*, 4686-4690.

[13] McQuade, T.J.; Tomasselli, A.G.; Liu, L.; Karacostas, B.; Moss, B.; Sawyer, T.K.; Heinrikson, R.L.; Tarpley, W.G. A synthetic HIV protease inhibitor with antiviral activity arrests HIV-like particle maturation. *Science*, **1990**, *247*, 454-456.

[14] Seelmeier, S.; Schmidt, H.; Turk, V.; von der Helm, K. Human immunodeficiency virus has an aspartic-type protease that can be inhibited by pepstatin A. *Proc. Natl. Acad. Sci. USA*, **1988**, *85*, 6612-616.

[15] Vacca, J.P.; Guare, J.P.; deSolms, S.J.; Sanders, W.M.; Giuliani, E.A.; Young, S.D.; Darke, P.L.; Zugay, J.; Sigal, I.S.; Schleif, W.A.; Quintero, J.C.; Emini, E.A.; Anderson, P.S.; Huff, J.R. L-687,908, a potent hydroxyethylene-containing HIV protease inhibitor. *J. Med. Chem.*, **1991**, *34*, 1225-1228.

[16] Vacca, J.P.; Condra, J.H. Clinically effective HIV-1 protease inhibitors. *Drug Discov. Today*, **1997**, *2*, 261-272.

[17] Roberts, N.A. Rational design of peptide-based HIV proteinase inhibitors. *Science*, **1990**, *248*, 358-361.

[18] Graves, B.J.; Hatada, M.H.; Miller, J.K.; Graves, M.C.; Roy, S.; Cook, C.M.; Krohn, A.; Martin, J.A.; Roberts, N.A. The three-dimensional x-ray crystal structure of HIV-1 protease complexed with a hydroxyethylene inhibitor. *Adv. Exp. Med. Biol.*, **1991**, *306*, 455-460.

[19] Krohn, A.; Redshaw, S.; Ritchie, J.C.; Graves, B.J.; Hatada, M.H. Novel binding mode of highly potent HIV-proteinase inhibitors incorporating the (*R*)-hydroxyethylamine isostere. *J. Med. Chem.*, **1991**, *34*, 3340-3342.

[20] Thompson, J.D.; Higgins, D.G.; Gibson, T.J. Improved sensitivity of profile searches through the use of sequence weights and gap excision. *Comput. Appl. Biosci.*, **1994**, *10*, 19-29.

[21] Seto, J.T.; Rott, R. Functional significance of sialidase during influenza virus multiplication. *Virology*, **1966**, *30*, 731-737.

[22] Palese, P.; Tobita, K.; Ueda, M.; Compans, R.W. Characterization of temperature sensitive influenza virus mutants defective in neuraminidase. *Virology*, **1974**, *61*, 397-410.

[23] Moscona A. Neuraminidase inhibitors for influenza. *N. Engl. J. Med.*, **2005**, *353*, 1363-1373.

[24] Varghese J.N.; Laver W.G.; Colman P.M. Structure of the influenza virus glycoprotein antigen neuraminidase at 2.9 Å resolution. *Nature*, **1983**, *303*, 35-40.

[25] von Itzstein, M.; Wu, W.–Y.; Kok, G.B.; Pegg, M.S.; Dyason, J.C.; Jin, B.; Phan, T.V.; Smythe, M.L.; White, H.F.; Oliver, S.W.; Colman, P.M.; Varghese, J.N.; Ryan, D.M.; Woods, J.M.; Bethell, R.C.; Hotham, V.J.; Cameron, J.M.; Penn, C.R. Rational design of potent sialidase-based inhibitors of influenza virus replication. *Nature*, **1993**, *363*, 418-423.

[26] Goodford, P.J. A computational procedure for determining energetically favorable binding sites on biologically important macromolecules. *J. Med. Chem.*, **1985**, *28*, 849-857.

[27] Abdel-Magid, A.F.; Maryanoff, C.A.; Mehrman, S.J. Synthesis of influenza neuraminidase inhibitors. *Curr. Opin. Drug Discov. Dev.*, **2001**, *4*, 776-791.

[28] Bossart-Whitaker, P.; Carson, M.; Babu, Y.S.; Smith, C.D.; Laver, W.G.; Air, G.M. Three-dimensional structure of influenza A N9 neuraminidase and its complex with the inhibitor 2-deoxy 2,3-dehydro-*N*-acetyl neuraminic acid. *J. Mol. Biol.*, **1993**, *232*, 1069-1083.

[29] Wood, J.M.; Bethell, R.C.; Coates, J.A.; Healy, N.; Hiscox, S.A.; Pearson, B.A.; Ryan, D.M.; Ticehurst, J.; Tilling, J.; Walcott, S.M. 4-Guanidino-2,4-dideoxy-2,3-dehydro-N-acetylneuraminic acid is a highly effective inhibitor both of the sialidase (neuraminidase) and of growth of a wide range of influenza A and B viruses *in vitro*. *Antimicrob. Agents Chemother.*, **1993**, *37*, 1473-1479.

[30] (a) Ryan, D.M.; Ticehurst, J.; Demsey, M.H.; Penn, C.R. Inhibition of influenza virus replication in mice by GG167 (4-guanidino-2,4-dideoxy-2,3-dehydro-N-acetylneuraminic acid) is consistent with extracellular activity of viral neuraminidase (sialidase). *Antimicrob. Agents Chemother.*, **1994**, *38*, 2270-2275. (b) Hayden, F.G.; Treanor, J.J.; Betts, R.F.; Lobo, M.; Esinhart, J.; Hussey, E.K. Safety and efficacy of the neuraminidase inhibitor GG167 in experimental human influenza. *J. Am. Med. Assoc.*, **1996**, *275*, 295-299.

[31] Kim, C.U.; Lew, W.; Williams, M.A.; Liu, H.; Zhang, L.; Swaminathan, S.; Bischofberger, N.; Chen, M.S.; Mendel, D.B.; Tai, C.Y.; Laver, W.G.; Stevens, R.C. Influenza neuraminidase inhibitors possessing a novel hydrophobic interaction in the enzyme active site: Design, synthesis, and structural analysis of carbocyclic sialic acid analogues with potent anti-influenza activity. *J. Am. Chem. Soc.*, **1997**, *119*, 681-690.

[32] Azizi, M.; Guyene, T.T.; Chatellier, G.; Menard, J. Blood pressure effects of acute intravenous renin or oral angiotensin converting enzyme inhibition in essential hypertension. *J. Hypertens.*, **1994**, *12*, 419-427.

[33] Wood, J.M.; Maibaum, J.; Rahuel, J.; Grutter, M.G.; Cohen, N.C.; Rasetti, V.; Ruger, H.; Goschke, R.; Stutz, S.; Fuhrer, W.; Schilling, W.; Rigollier, P.; Yamaguchi, Y.; Cumin, F.; Baum, H.P.; Schnell, C.R.; Herold, P.; Mah, R.; Jensen, C.; O'Brien, E.; Stanton, A.; Bedigianj, M.P. Structure-based design of Aliskiren, a novel orally effective renin inhibitor. *Biochem. Biophys. Res. Commun.*, **2003**, *308*, 698-705.

[34] Wolfenden, R. Analog approaches to the structure of the transition state in enzyme reactions. *Acc. Chem. Res.*, **1972**, *5*, 10-18.

[35] Rahuel, J.; Priestle, J.P.; Grutter, M.G. The crystal structures of recombinant glycosylated human renin alone and in complex with a transition state analog inhibitor. *J. Struct. Biol.*, **1991**, *107*, 227-236.

[36] Cohen, N.C. Structure-based drug design and the discovery of Aliskiren (Tekturna): Perseverance and creativity to overcome a R&D pipeline Challenge. *Chem. Biol. Drug Des.*, **2007**, *70*, 557-565.

[37] Goschke, R.; Cohen, N.C.; Wood, J.M.; Maibaum, J. Design and synthesis of novel 2,7-dialkyl substituted 5(*S*)-amino-4(*S*)-hydroxy-8-phenyl-octanecarboxamides as *in vitro* potent peptidomimetic inhibitors of human renin. *Bioorg. Med. Chem. Lett.*, **1997**, *7*, 2735-2740.

[38] Rahuel, J.; Rasetti, V.; Maibaum, J.; Ruger, H.; Goschke, R.; Cohen, N.C.; Stutz, S.; Cumin, F.; Fuhrer, W.; Wood, J.M.; Grutter, M.G. Structure-based drug design: the discovery of novel nonpeptide orally active inhibitors of human renin. *Chem. Biol.*, **2000**, *7*, 493-504.

[39] (a) Lamarre, D.; Anderson, P.C.; Bailey, M.; Beaulieu, P.; Bolger, G.; Bonneau, P.; Bös, M.; Cameron, D.R.; Cartier, M.; Cordingley, M.G.; Faucher, A.-M.; Goudreau, N.; Kawai, S.H.; Kukolj, G.; Lagacé, L.; LaPlante, S.R.; Narjes, H.; Poupart, M.-A; Rancourt, J.; Sentjens, R.E.; George, T.S.; Simoneau, B.; Steinmann, G.; Thibeault, D.; Tsantrizos, Y.S.; Weldon, S.M.; Yong, C.-L.; Llinàs-Brunet, M. An NS3 protease inhibitor with antiviral effects in humans infected with hepatitis C virus. *Nature*, **2003**, *426*, 186-189. (b) Perni, R.B.; Almquist, S.J.; Byrn, R.A.; Chandorkar, G.; Chaturvedi, P.R.; Courtney, L.F.; Decker, C.J.; Dinehart, K.; Gates, C.A.; Harbeson, S.L.; Heiser, A.; Kalkeri, G.; Kolaczkowski, E.; Lin, K.; Luong, Y.-P.; Rao, B. G.; Taylor, W.P.; Thomson, J.A.; Tung, R.D.; Wei, Y.; Kwong, A.D.; Lin, C. Preclinical profile of VX-950, a potent, selective, and orally, bioavailable inhibitor of hepatitis C virus NS3-NS4A serine protease. *Antimicrob. Agents Chemother.*, **2006**, *50*, 899-909.

[40] De Francesco, R.; Migliaccio, G. Challenges and successes in developing new therapies for hepatitis C. *Nature*, **2005**, *436*, 953-960.

[41] Njoroge, F.G.; Chen, K.X.; Shih, N.–Y.; Piwinski, J.P. Challenges in modern drug discovery: A case study of boceprevir, an HCV protease inhibitor for the treatment of hepatitis C virus infection. *Acc. Chem. Res.*, **2008**, *41*, 50-59.

[42] (a) Turk, B. Targeting proteases: Successes, failures and future prospects. *Nat. Rev. Drug Discov.*, **2006**, *5*, 785-799. (b) Tyndall, J.D.; Nall, T.; Fairlie, D.P. Proteases universally recognize beta strands in their active sites. *Chem. Rev.*, **2005**, *105*, 973-999. (c)

Powers, J.C.; Asgian, J.L.; Ekici, D.; James, K.E. Irreversible inhibitors of serine, cysteine, and threonine proteases. *Chem. Rev.*, **2002**, *102*, 4639-4643. (d) Leung, D.; Abbenante, G.; Fairlie, D.P. Protease inhibitors: Current status and future prospects. *J. Med. Chem.*, **2000**, *43*, 305-341.

[43] (a) Yan, Y.; Li, Y.; Munshi, S.; Sardana, V.; Cole, J.L.; Sardana, M.; Steinkuehler, C.; Tomei, L.; De Francesco, R.; Kuo, L.C.; Chen, Z. Complex of NS3 protease and NS4A peptide of BK strain hepatitis C virus: A 2.2 Å resolution structure in a hexagonal crystal form. *Protein Sci.*, **1998**, *7*, 837-847. (b) Love, R.A.; Parge, H.E.; Wichersham, J.A.; Hostomsky, Z.; Habuka, N.; Moomaw, E.W.; Adachi, T.; Hostomska, Z. The crystal structure of hepatitis C virus NS3 proteinase reveals a trypsin-like fold and a structural zinc binding site. *Cell*, **1996**, *87*, 331-342.

[44] (a) Venkatraman, S.; Bogen, S.L.; Arasappan, A.; Bennett, F.; Chen, K.; Jao, J.; Liu, Y.-T.; Lovey, R.; Hendrata, S.; Huang, Y.; Pan, W.; Parekh, T.; Pinto, P.; Popov, V.; Pike, R.; Ruan, S.; Santhanam, B.; Vibulbhan, B.; Wu, W.; Yang, W.; Kong, J.; Liang, X.; Wong, J.; Liu, R.; Butkiewicz, N.; Chase, R.; Hart, A.; Agrawal, S.; Ingravallo, P.; Pichardo, J.; Kong, R.; Baroudy, B.; Malcolm, B.; Guo, Z.; Prongay, A.; Madison, V.; Broske, L.; Cui, X.; Cheng, K.-C.; Hsieh, Y.; Brisson, J.-M.; Prelusky, D.; Korfmacher, W.; White, R.; Bogdanowich-Knipp, S.; Pavlovsky, A.; Bradley, P.; Saksena, A.K.; Ganguly, A.; Piwinski, J.; Girijavallabhan, V.; Njoroge, F.G. Discovery of (1*R*,5*S*)-*N*-[3-amino-1-(cyclobutylmethyl)-2,3-dioxopropyl]-3-[2(*S*)-[[[(1,1-dimethylethyl)amino]carbonyl]amino]-3,3-dimethyl-1-oxobutyl]-6,6-dimethyl-3-azabicyclo[3.1.0]hexan-2(*S*)-carboxamide (SCH 503034), a selective, potent, orally bioavailable hepatitis C virus NS3 protease inhibitor: A potential therapeutic agent for the treatment of hepatitis C infection. *J. Med. Chem.*, **2006**, *49*, 6074-6086. (b) Malcolm, B.A.; Liu, R.; Lahser, F.; Agrawal, S.; Belanger, B.; Butkiewicz, N.; Chase, R.; Gheyas, F.; Hart, A.; Hesk, D.; Ingravallo, P.; Jiang, C.; Kong, R.; Lu, J.; Pichardo, J.; Prongay, A.; Skelton, A.; Tong, X.; Venkatraman, S.; Xia, E.; Girijavallabhan, V.; Njoroge, F.G. SCH 503034, a mechanism-based inhibitor of hepatitis C virus NS3 protease, suppresses polyprotein maturation and enhances the antiviral activity of alpha interferon in replicon cells. *Antimicrob. Agents Chemother.*, **2006**, *50*, 1013-1020.

[45] Schechter, I.; Berger, A. On the size of the active site in proteases. I. Papain. *Biochem. Bioph. Res. Commun.*, **1967**, *27*, 157-162.

[46] Webber, S.E.; Bleckman, T.M.; Attard, J.; Deal, J.G.; Kathardekar, V.; Welsh, K.M.; Webber, S.; Janson, C.A.; Matthews, D.A.; Smith, W.W.; Freer, S.T.; Jordan, S.R.; Bacquet, R. J.; Howland, E.F.; Booth, C.L.J.; Ward, R.W.; Hermann, S.M.; White, J.; Morse, C.A.; Hilliard, J.A.; Bartlett, C.A. Design of thymidylate synthase inhibitors using protein crystal structures: The synthesis and biological evaluation of a novel class of 5-substituted quinazolinones. *J. Med. Chem.*, **1993**, *36*, 733-746.

[47] Jones, T.R.; Calvert, A.H.; Jackman, A.L.; Brown, S.J.; Jones, M.; Harrap, K.R. A potent antitumor quinazoline inhibitor of thymidylate synthetase: synthesis, biological properties and therapeutic results in mice. *Eur. J. Cancer*, **1981**, *17*, 11-19.

[48] Matthews, D.A.; Appelt, K.; Oatley, S.J.; Xuong, N.H. Crystal structure of Escherichia coli thymidylate synthase containing bound 5-fluoro-2'-deoxyuridylate and 10-propargyl-5,8-dideazafolate. *J. Mol. Biol.*, **1990**, *214*, 923-936.

[49] Black, R.A.; Rauch, C.T.; Kozlosky, C.J.; Peschon, J.J.; Slack, J.L.; Wolfson, M.F.; Castner, B.J.; Stocking, K.L.; Reddy, P.; Srinivasan, S.; Nelson, N.; Boiani, N.; Schooley, K.A.; Gerhart, M.; Davis, R.; Fitzner, J.N.; Johnson, R.S.; Paxton, R.J.; March, C.J.; Cerretti, D.P. A metalloproteinase disintegrin that releases tumour-necrosis factor-alpha from cells. *Nature*, **1997**, *385*, 729-733.

[50] Vassalli, P. The pathophysiology of tumor necrosis factors. *Ann. Rev. Immunol.*, **1992**, *10*, 411-452.

[51] Maskos, K.; Fernandez-Catalan, C.; Huber, R.; Bourenkov, G.P.; Bartunik, H.; Ellestad, G.A.; Reddy, P.; Wolson, M.F.; Rauch, C.T.; Castner, B.J.; Davis, R.; Clarke, H.R.G.; Petersen, M.; Fitzner, J.N.; Cerretti, D.P.; March, C.J.; Paxton, R.J.; Black, R.A.; Bode, W. Crystal structure of the catalytic domain of human tumor necrosis factor-R converting enzyme. *Proc. Natl. Acad. Sci. USA*, **1998**, *95*, 3408-3412.

[52] Levin, J.I.; Chen, J.M.; Cheung, K.; Cole, D.; Crago, C.; Delos Santos, E.; Du, X.; Khafizova, G.; MacEwan, G.; Niu, C.; Salaski, E. J.; Zask, A.; Cummons, T.; Sung, A.; Xu, J.; Zhang, Y.; Xu, W.; Ayral-Kaloustian, S.; Jin, G.; Cowling, R.; Barone, D.; Mohler, K.M.; Black, R.A.; Skotnicki, J.S. Acetylenic TACE inhibitors. Part 1. SAR of the acyclic sulfonamide hydroxamates. *Bioorg. Med. Chem. Lett.*, **2003**, *13*, 2798-2803.

[53] Levin, J.I.; Chen, J.M.; Laakso, L.M.; Du, M.; Schmid, J.; Xu, W.; Cummons, T.; Xu, J.; Jin, G.; Barone, D.; Skotnicki, J.S. Acetylenic TACE inhibitors. Part 3. Thiomorpholine sulfonamide hydroxamates. *Bioorg. Med. Chem. Lett.*, **2006**, *16*, 1605-1609.

[54] Liebeschuetz, J.W.; Jones, S.D.; Morgan, P.J.; Murray, C.W.; Rimmer, A.D.; Roscoe, J.M.; Waszkowycz, B.; Welsh, P.M.; Wylie, W.A.; Young, S.C.; Martin, H., Mahler, J.; Brady, L.; Wilkinson, K. PRO_SELECT: combining structure-based drug design and array-based chemistry for rapid lead discovery. 2. The development of a series of highly potent and selective factor Xa inhibitors. *J. Med. Chem.*, **2002**, *45*, 1221-1232.

[55] Jones, S.D.; Liebeschuetz, J.W.; Morgan, P.J.; Murray, C.W.; Rimmer, A.D.; Roscoe, J.M.; Waszkowycz, B.; Welsh, P.M.; Wylie, W.A.; Young, S.C.; Martin, H.; Mahler, J.; Brady, L.; Wilkinson, K. The design of phenylglycine containing benzamidine carboxamides as potent and selective inhibitors of Factor Xa. *Bioorg. Med. Chem. Lett.*, **2001**, *11*, 733-736.

[56] Agnelli, G.; Haas, S.; Ginsberg, J.S.; Krueger, K.A.; Dmitrienko, A.; Brandt, J.T. A phase II study of the oral factor Xa inhibitor LY517717 for the prevention of venous thromboembolism after hip or knee replacement. *J. Thromb. Haemost.*, **2007**, *5*, 746-753.

[57] (a) Orr, D.C.; Long, A.C.; Kay, J.; Dunn, B.M.; Cameron, J.M. Hydrolysis of a series of synthetic peptide substrates by the human rhinovirus 14 3C proteinase, cloned and expressed in *Escherichia coli*. *J. Gen. Virol.*, **1989**, *70*, 2931-2942. (b) Cordingley, M.G.; Register, R.B.; Callahan, P.L.; Garsky, V.M.; Colonno, R.J. Cleavage of small peptides *in vitro* by human rhinovirus 14 3C protease expressed in *Escherichia coli*. *J. Virol.*, **1989**, *63*, 5037-5045.

[58] Long, A.C.; Orr, D.C.; Cameron, J.M.; Dunn, B.M.; Kay, J. A consensus sequence for substrate hydrolysis by rhinovirus 3C proteinase. *FEBS Lett.*, **1989**, *258*, 75-78.

[59] Malcolm, B.A.; Lowe, C.; Shechosky, S.; Mckay, R.T.; Yang, C.C.; Shah, V.J.; Simon, R. J.; Vederas, J.C.; Santi, D.V. Peptide aldehyde inhibitors of hepatitis A virus 3C proteinase. *Biochemistry*, **1995**, *34*, 8172-8179.

[60] Shepherd, T.A.; Cox, G.A.; McKinney, E.; Tang, J.; Wakulchik, M.; Zimmerman, R.E.; Villarreal, E.C. Small peptidic aldehyde inhibitors of human rhinovirus 3C protease. *Bioorg. Med. Chem. Lett.*, **1996**, *6*, 2893-2896.

[61] Webber, S.E.; Okano, K.; Little, T.L.; Reich, S.H.; Xin, Y.; Fuhrman, S.A.; Matthews, D. A.; Love, R.A.; Hendrickson, T.F.; Patick, A.K.; III, Meador, J.W. III; Ferre, R.A.; Brown, E.L.; Ford, C.E.; Binford, S.L.; Worland, S.T. Tripeptide aldehyde inhibitors of human rhinovirus 3C protease: design, synthesis, biological evaluation, and cocrystal structure solution of P1 glutamine isosteric replacements. *J. Med. Chem.*, **1998**, *41*, 2786-2805.

[62] Kaldor, S.W.; Hammond, M.; Dressman, B.A.; Labus, J.M.; Chadwell, F.W.; Kline, A.D.; Heinz, B.A. Glutamine-derived aldehydes for the inhibition of human rhinovirus 3C protease. *Bioorg. Med. Chem. Lett.*, **1995**, *5*, 2021-2026.

[63] Matthew, D.A.; Dragovich, P.S.; Webber, S.E.; Fuhrman, S.A.; Patick, A.K.; Zalman, L.S.; Hendrickson, T.F.; Love, R.A.; Prins, T.J.; Marakovits, J.T.; Zhou, R.; Tikhe, J.; Ford, C.E.; Meador, J.W.; Ferre, R.A.; Brown, E.L.; Binford, S.L.; Brothers, M.A.; Delisle, D.M.; Worland, S.T. Structure-assisted design of mechanism-based irreversible inhibitors of human rhinovirus 3C protease with potent antiviral activity against multiple rhinovirus serotypes. *Proc. Natl. Acad. Sci. USA*, **1999**, *96*, 11000-11007.

[64] Dragovich, P.S.; Webber, S.E.; Babine, R.E.; Fuhrman, S.A.; Patick, A.K.; Matthews, D. A.; Reich, S.H.; Marakovits, J.T.; Prins, T.J.; Zhou, R. Structure-based design, synthesis, and biological evaluation of irreversible human rhinovirus 3C protease inhibitors. 2. Peptide structure-activity studies. *J. Med. Chem.*, **1998**, *41*, 2819-2834.

[65] Dragovich, P.S.; Webber, S.E.; Babine, R.E.; Fuhrman, S.A.; Patick, A.K.; Matthews, D.A.; Lee, C.A.; Reich, S.H.; Prins, T.J.; Marakovits, J.T. Structure-based design, synthesis, and biological evaluation of irreversible human rhinovirus 3C protease inhibitors. 1. Michael acceptor structure-activity studies. *J. Med. Chem.*, **1998**, *41*, 2806-2818.

[66] Dragovich, P.S.; Webber, S.E.; Babine, R.E.; Fuhrman, S.A.; Patick, A.K.; Matthews, D.A.; Reich, S.H.; Marakovits, J.T.; Prins, T.J.; Zhou, R. Structure-based design, synthesis, and biological evaluation of irreversible human rhinovirus 3C protease inhibitors. 4. Incorporation of P1 lactam moieties as L-glutamine replacements. *J. Med. Chem.,* **1999**, *42*, 1213-1224.

[67] Dragovich, P.S.; Prins, T.J.; Zhou, R.; Fuhrman, S.A.; Patick, A.K.; Matthews, D.A.; Ford, C.E.; Meador, J.W.; Ferre, R.A.; Worland, S.T. Structure-based design, synthesis, and biological evaluation of irreversible human rhinovirus 3C protease inhibitors. 3. Structure-activity studies of ketomethylene-containing peptidomimetics. *J. Med. Chem.*, **1999**, *42*, 1203-1212.

[68] Dragovich, P.S.; Zhou, R.; Skalitzky, D.J.; Fuhrman, S.A.; Patick, A.K.; Ford, C.E.; Meador, J.W.; Worland, S.T. Solid-phase synthesis of irreversible human rhinovirus 3C protease inhibitors. Part 1: Optimization of tripeptides incorporating N-terminal amides. *Bioorg. Med. Chem.*, **1999**, *7*, 589-598.

[69] Patick, A.K.; Binford, S.L.; Brothers, M.A.; Jackson, R.L.; Ford, C.E.; Diem, M.D.; Maldonado, F.; Dragovich, P.S.; Zhou, R.; Prins, T.J.; Fuhrman, S.A.; Meador, J.W.; Zalman, L.S.; Matthews, D.A.; Worland, S.T. *In vitro* antiviral activity of AG7088, a potent inhibitor of human rhinovirus 3C protease. *Antimicrob. Agents Chemother*., **1999**, *43*, 2444-2450.

[70] Patick, A.K. Rhinovirus chemotherapy. *Antiviral Res.,* **2006**, *71*, 391-396.

[71] Sharp, S.; Workman, P. Inhibitors of the HSP90 molecular chaperone: current status. *Adv. Cancer Res.*, **2006**, *95*, 323-328.

[72] Whitesell, L.; Lindquist, S.L. HSP90 and the chaperoning of cancer. *Nat. Rev. Cancer,* **2005**, *5*, 761-772.

[73] Workman, P.; Burrows, F.; Neckers, L.; Rosen, N. Drugging the cancer chaperone HSP90: combinatorial therapeutic exploitation of oncogene addiction and tumor stress. *Ann. N. Y. Acad. Sci.,* **2007**, *1113*, 202-216.

[74] Pearl, L.H.; Prodromou, C. Structure and mechanism of the Hsp90 molecular chaperone machinery. *Ann. Rev. Biochem.,* **2006**, *75*, 271-294.

[75] Cheung, K.M.; Matthews, T.P.; James K.; Rowlands M.G.; Boxall, K.J.; Sharp, S.Y.; Maloney, A.; Roe, S.M.; Prodromou, C.; Pearl, L.H.; Aherne, G.W.; McDonald, E.; Workman, P. The identification, synthesis, protein crystal structure and *in vitro* biochemical evaluation of a new 3,4-diarylpyrazole class of Hsp90 inhibitors. *Bioorg. Med. Chem. Lett.,* **2005**, *15*, 3338-3343.

[76] Sharp, S.Y.; Rowlands, M.; Prodromou, C.S.; Roe, S.M.; Maloney, A.; Powers, M.; Clarke, P.A.; Box, G.; Sanderson, S.; Patterson, L.; Matthews, T.P.; Cheung, K.M.; Ball, K.; Hayes, A.; Raynaud, F.; Marais, R.; Pearl, L.; Eccles, S.; Aherne, W.; McDonald, E.; Workman, P. *In vitro* biological characterization of a novel, synthetic diaryl pyrazole resorcinol class of HSP90 inhibitors. *Cancer Res*., **2007**, *67*, 2206-2216.

[77] Smith, N.F.; Hayes, A.; James, K.; Nutley, B.P.; McDonald, E.; Henley, A.; Dymock, B.; Drysdale, M.J.; Raynaud, F.I.; Workman, P. Preclinical pharmacokinetics and metabolism of a novel diaryl pyrazole resorcinol series of heat shock protein 90 inhibitors. *Mol. Cancer Ther.,* **2006**, *5*, 1628-1637.

[78] Dymock, B.W.; Barril, X.; Brough, P.A.; Cansfield, J.E.; Massey, A.; McDonald, E.; Hubbard, R.E.; Surgenor, A.; Roughley, S.D.; Webb, P.; Workman, P.; Wright, L.; Drysdale, M.J. Novel, potent small-molecule inhibitors of the molecular chaperone Hsp90 discovered through structure-based design. *J. Med. Chem.,* **2005**, *48*, 4212-4215.

[79] Sharp, S.Y.; Prodromou, C.; Boxall, K.; Powers, M.V.; Holmes, J.L.; Box, G.; Matthews, T.P.; Cheung, K.M.; Kalusa, A.; James, K.; Hayes, A.; Hardcastle, A.; Dymock, B.; Brough, P.A.; Barril, X.; Cansfield, J.E.; Wright, L.; Surgenor, A.; Foloppe, N.; Hubbard, R.E.; Aherne, W.; Pearl, L.; Jones, K.; McDonald, E.; Raynaud, F.; Eccles, S.; Drysdale, M.; Workman, P. Inhibition of the heat shock protein 90 molecular chaperone *in vitro* and *in vivo* by novel, synthetic, potent resorcinylic pyrazole/isoxazole amide analogues. *Mol. Cancer Ther.,* **2007**, *6*, 1198-1211.

[80] Brough, P.A.; Aherne, W.; Borgognoni, J.; Boxall, K.; Cansfield, J.E.; Cheung, K.M.; Collins, I.; Davies, N.G.; Drysdale, M.J.; Dymock, B.; Eccles, S.A.; Finch, H.; Fink, A.; Hayes, A.; Howes, R.; Hubbard, R.E.; James, K.; Jordan, A.M.; Lockie, A.; Martins, V.; Massey, A.; Matthews, T.P.; McDonald, E.; Northfield, C.J.; Pearl, L.H.; Prodromou, C.; Ray, S.; Raynaud, F.I.; Roughley, S.D.; Sharp, S.Y.; Surgenor, A.; Walmsley, D.L.; Webb, P.; Wood, M.; Workman, P.; Wright, L. 4,5-Diarylisoxazole Hsp90 chaperone inhibitors: potential therapeutic agents for the treatment of cancer. *J. Med. Chem.,* **2008**, *51*, 196-218.

[81] Eccles, S.A.; Massey, A.; Raynaud, F.I.; Sharp, S.Y.; Box, G.; Valenti, M.; Patterson, L.; Brandon, A.H.; Gowan, S.; Boxall, F.; Aherne, W.; Rowlands, M.; Hayes, A.; Martins, V.; Urban, F.; Boxall, K.; Prodromou, C.; Pearl, L.; James, K.; Matthews, T.P.; Cheung, K.M.; Kalusa, A.; Jones, K.; McDonald, E.; Barril, X.; Brough, P.A.; Cansfield, J.E.; Dymock, B.; Drysdale, M.J.; Finch, H.; Howes, R.; Hubbard, R.E.; Surgenor, A.; Webb, P.; Wood, M.; Wright, L.; Workman, P. NVP-AUY922: A novel heat shock protein 90 inhibitor active against xenograft tumor growth, angiogenesis, and metastasis. *Cancer Res.*, **2008**, *68*, 2850-2860.

[82] Caldwell, J.J.; Davies, T.G.; Donald, A.; McHardy, T.; Rowlands, M.G.; Aherne, G.W.; Hunter, L.K.; Taylor, K.; Ruddle, R.; Raynaud, F.I.; Verdonk, M.; Workman, P.; Garrett, M.D.; Collins, I. Identification of 4-(4-aminopiperidin-1-yl)-7H-pyrrolo[2,3-d]pyrimidines as selective inhibitors of protein kinase B through fragment elaboration. *J. Med. Chem.,* **2008**, *51*, 2147-2157.

Received: August 4, 2009 Revised: August 21, 2009